STUDY OF HIGH-PERFORMANCE MPPT ALGORITHMS FOR BIPV APPLICATIONS

Ana-Maria BADEA[1], Doina MANAILA- MAXIMEAN[2,3], Dan CRACIUNESCU[4, *]

Evaluating the electrical performance of photovoltaic (PV) systems and optimizing their energy output remains challenging due to the variability of meteorological conditions. This study presents a unified approach to the operational optimization of BIPV systems, relying on methodologies and tools commonly used for PV system design. While these tools provide valuable insights, they are often insufficient for detailed assessment under real-world operating conditions, as they may not capture critical phenomena such as partial shading or the effect of bypass diodes on system protection and energy stability.

In this work, the performance of BIPV systems is analyzed with particular focus on the efficiency of Maximum Power Point Tracking (MPPT) algorithms under both partial and extreme shading scenarios. Hourly measured data were used to evaluate the specific energy yield (kWh/kWp), demonstrating the adaptability of MPPT algorithms to dynamic environmental conditions. The study further highlights the importance of bypass diodes for system protection and emphasizes the need to integrate advanced MPPT strategies to maximize the overall efficiency of PV generators.

Keywords: Photovoltaic, MPPT, Numerical Modeling, Simulation, Partial Shading, Bypass Diodes, Meteorological Parameters, Shockley Equation

1. Introduction

In the current context, marked by the transition to sustainable energy sources and the pressures generated by the fossil fuel crisis, photovoltaic (PV) systems are emerging as one of the most viable solutions for the production of clean and efficient energy [1–13]. However, simplified theoretical analysis alone is insufficient for a rigorous evaluation of system performance, as it must also consider meteorological factors and advanced optimization models [14–19]. Solar

[1] PhD candidate, Faculty of Applied Sciences, National University of Science and Technology POLITEHNICA Bucharest, Romania, e-mail: ana_maria.badea1210@stud.fsa.upb.ro

[2] Professor, PhD, Faculty of Applied Sciences, National University of Science and Technology POLITEHNICA Bucharest, Romania, e-mail: doina.manaila@upb.ro

[3] Academy of Romanian Scientists, 3 Ilfov Str., RO-050094 Bucharest, Romania

[4]* Lecturer Dr., Faculty of Applied Sciences, The National University of Science and Technology POLITEHNICA Bucharest, Romania, email: dan.craciunescu@upb.ro (Corresponding author)

irradiation plays a crucial role in determining the energy generated by the PV panels, but their performance does not depend exclusively on this parameter.

Ambient temperature and wind conditions significantly influence the efficiency of energy conversion, through the impact on the thermal operating scenarios of the modules. Thus, an integrated analysis of these variables allows a more accurate understanding of the behavior of PV systems under real operating conditions and contributes to obtaining more accurate operational optimization, adapted to dynamic shifts.

2. Theoretical background

2.1. Model of PV cells under Partial Shading

For description of the electrical behavior of a solar cell, the two diodes model is used (see Fig. 1a). More involved approaches, derived from the two-diode model, take account of the cases where negative voltages for solar cells can occur at non-uniform illuminated photovoltaic generators, especially during partial shading of the cell [28, 29].

The electrical behavior of a solar cell can be described using the two-diode model, which accounts for recombination effects and partial shading. The cell current $\boldsymbol{I_{cell}}$ is expressed as:

$$\boldsymbol{I_{cell} = I_{ph}(x,y) - (I_{D1} + I_{D2}) - I_{sh}(x,y)} \quad (1)$$

The voltage V over the shunt resistance $\boldsymbol{R_{sh}}$ is given by $V = V_{cell} + R_s I_{cell}$,

$$\boldsymbol{V = V_{cell} + R_s I_{cell}, I_{sh} = \frac{V}{R_{sh}}} \quad (2)$$

Where: $\boldsymbol{I_{ph}(x,y)}$is the locally photo-generated current, dependent on irradiance distribution, $\boldsymbol{I_{D1}}$and $\boldsymbol{I_{D2}}$are the currents through the ideal and recombination diodes, respectively, $\boldsymbol{I_{sh}(x,y)}$is the shunt current through regions with non-uniform illumination, $\boldsymbol{V_{cell}}$ is the voltage across the cell, $\boldsymbol{R_s}$ is the series resistance; $\boldsymbol{R_{sh}}$ is the shunt resistance.

The diode currents follow the Shockley equation:

$$\boldsymbol{I_{D1,2} = I_{0,1/2}\left[\exp\left(\frac{V_{cell}+R_s I_{cell}}{n_{1/2}V_T}\right) - 1\right]} \quad (3)$$

Where: $\boldsymbol{I_{0,1/2}}$are the saturation currents, $\boldsymbol{n_{1,2}}$ the diode ideality factors, $\boldsymbol{V_T = kT_{cell}/q}$ the thermal voltage, $\boldsymbol{q}$ the electron charge, $\boldsymbol{k}$ Boltzmann's constant, and $\boldsymbol{T_{cell}}$the cell temperature.

For silicon solar cells, the photocurrent and saturation currents can be approximated by:

$$I_{ph} = G_T(\tau\alpha)_s A_{cell} \tag{4}$$

$$I_0 = K_{cell} A_{cell} T_{cell}^3 \exp\left(-\frac{E_g}{kT_{cell}}\right) \tag{5}$$

Where: G_T is the global irradiance on the cell, $(\tau\alpha)_s$ the effective transmittance–absorptance product, A_{cell} the cell area, K_{cell} a material constant, and E_g the silicon bandgap.

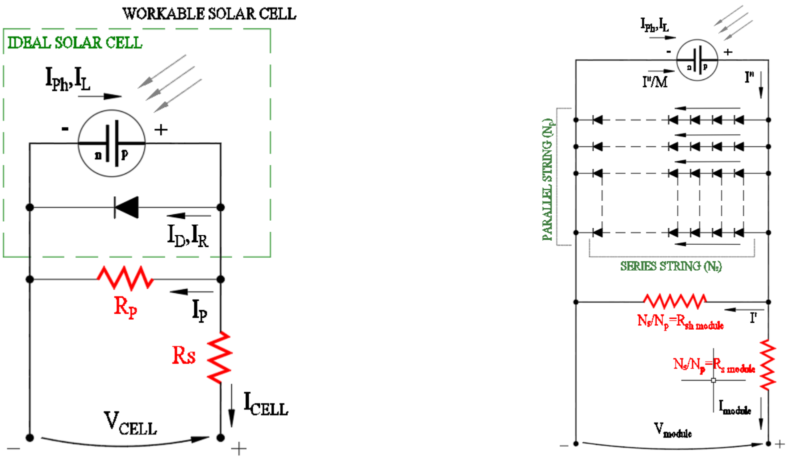

(a) (b)

Fig. 1. (a) PV cell electrical model. S and D—photo-sensible and diode-type components of solar cell. R_s, R_{sh}—series and shunt resistance, respectively; (b) Electrical model of a simple series–parallel PV module. $R_{s,module}$, $R_{sh,module}$—series and shunt resistance, respectively.

2.2. Photovoltaic Module Model under Partial Shading

The method developed in this paper considers a simple series–parallel configuration but can be extended to other interconnection schemes. A PV module consists of M parallel strings, each containing N identical solar cells (Fig. 1b). The relation between the cell voltage V_{cell} and the module voltage V_{module} is:

$$V_{cell} = \frac{V_{module} + I_{module} R_{s,module}}{N} \tag{6}$$

where $R_{s,module}$ is the module series resistance. The shunt current through the module shunt resistance $R_{sh,module}$ is:

$$I' = \frac{V_{module} + I_{module} R_{s,module}}{R_{sh,module}} \tag{7}$$

And the total module current I'' is given by:

$$I'' = I_{cell} M = I_{module} + I' \tag{8}$$

Using the solar cell two-diode model (Sec. 2.1) and Eqs. (2.6) – (2.8), the PV module current–voltage relation becomes:

$$I_{module} = MI_{ph} - M(I_{D1} + I_{D2}) - I' \tag{9}$$

With

$$I_{D1,2} = I_{0,1/2}\left[\exp\left(\frac{V_{cell} + R_s I_{cell}}{n_{1/2}V_T}\right) - 1\right], V_{cell} = \frac{V_{module} + I_{module}R_{s,module}}{N}$$

Eq. (2.9) is an improved version of the classical module model [16], accounting for the module shunt resistance $R_{sh,module}$. The module power is:

$$P_{module} = I_{module}V_{module} \tag{10}$$

The energy balance for the entire module is:

$$MNA_{cell}G_T(\tau\alpha)_s - MNA_{cell}U_{cell}(T_{cell} - T_a) - I_{module}V_{module} = 0 \tag{11}$$

where $U_{cell}$and $T_{cell}$are average module values of the convective heat transfer coefficient and cell temperature, and $T_a$is ambient temperature. The first term represents solar energy absorbed by the module, the second term represents convective heat losses (including Joule heating in module resistances), and the third term is the electrical energy extracted.

The PV module efficiency is defined as:

$$\eta = \frac{P_{module}}{G_T A_{module}} \tag{12}$$

where the PV module area is given by $A_{module} = MNA_{cell}$

The model provides a rigorous framework for simulating PV module performance under non-uniform illumination, fully accounting for series and shunt losses.

3. Correlation of Meteorological Parameters with Photovoltaic Energy Production: Experimental Study and Modeling

In this chapter, the authors analyzed the energy produced by a PV panel used in a building-integrated photovoltaic (BIPV) architecture, in correlation with meteorological parameters, as well as their influence on the panel's actual performance. This approach enabled the assessment of the accuracy and limitations of the models used to describe the real energy behavior of PV systems [30].

Fig. 2 presents the conceptual diagram of a BIPV system consisting of PV panels with nominal power of 410 Wp. For the analysis, a single PV panel was considered, and the PV Lighthouse platform [31], which integrates software tools dedicated to photovoltaic systems, was used for modeling. The SISIFO application [32], suitable for modeling and simulating PV systems in various specific applications, was also used.

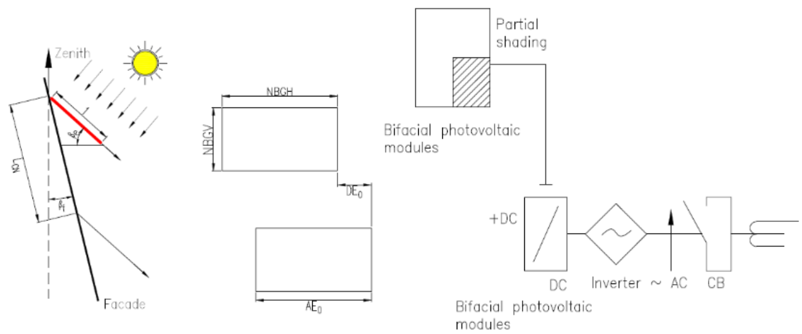

Fig. 2. Conceptual structure of a Building-Integrated Photovoltaic System (BIPV): AE_O – PV width ratio, DE_O - deviation ratio of the supporting structure, βG - generator inclination angle, βF - façade inclination angle, LCN - module separation ratio, zenith–nadir direction,

3.1.Input Data: Meteorological Parameters

The meteorological parameters were obtained from the SISIFO application, which integrates satellite databases and numerical weather forecast models, allowing the simulation and estimation of short- and medium-term atmospheric conditions, using advanced algorithms for detailed analysis of climate data and for improving the accuracy of forecasts.

A. Solar radiation: The data considered for the analysis covered a one-month period (June 1–29, 2023), with both daily and hourly resolution. The data indicated a daily average global horizontal irradiation varying between 5.5 and 8.5 kWh/m², without sudden fluctuations.

Fig. 3 shows the daily evolution of solar irradiation during the period June 1–29, expressed in kWh/m². The radiation curves represented in the graph correspond to 1) horizontal irradiance, i.e. the global value measured on a horizontal plane; 2) incident irradiance, i.e. the total radiation received on the tilted surface of the panels; and 3) effective irradiance, representing the useful energy, corrected for the orientation and tilted of the system. Horizontal irradiance values reached a maximum of over 8.5 kWh/m² on June 7, 22 and 23, which directly corresponds to the high levels of energy production shown on Fig. 8.

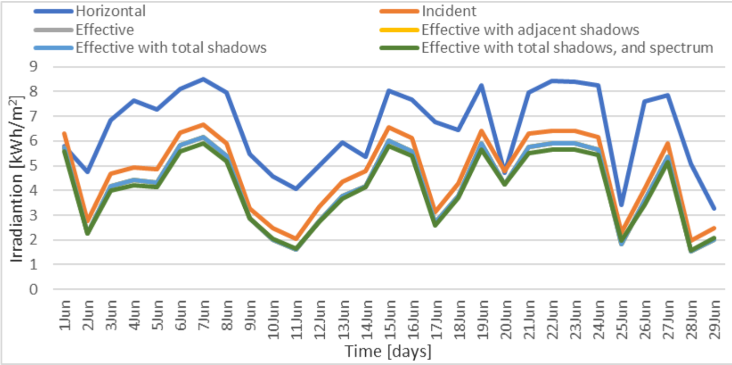

Fig. 3. Daily Solar Radiation Values, Including Their Specific Components

The minimum values were observed on June 2, 11, 17, 25, and 28, when irradiance decreased below 4 kWh/m², resulting in corresponding dropped in daily efficiency and energy output. The differences between incident and effective irradiance, particularly under shading and spectral variations, indicate significant losses, estimated between 10÷25% on the affected days. The daily representation provides an overall picture of available solar energy but may mask important intraday variations. In contrast, Fig. 4 and Fig. 5, which present hourly profiles, clearly highlight the dynamics of the energy flow and enable a detailed analysis. The hourly representation allows the identification of periods of reduced or absent radiation caused by (1) the presence of clouds or rapidly changing meteorological conditions, (2) shading from obstacles, and (3) the beginning and end of the day. These variations are not apparent in aggregated daily values, which may mask occasional drops in performance that are offset by higher radiation during other periods of the day.

By correlating hourly irradiance with energy production allows evaluation of system behavior under fluctuating conditions, responses to shading, and deviations between irradiance and generated energy.

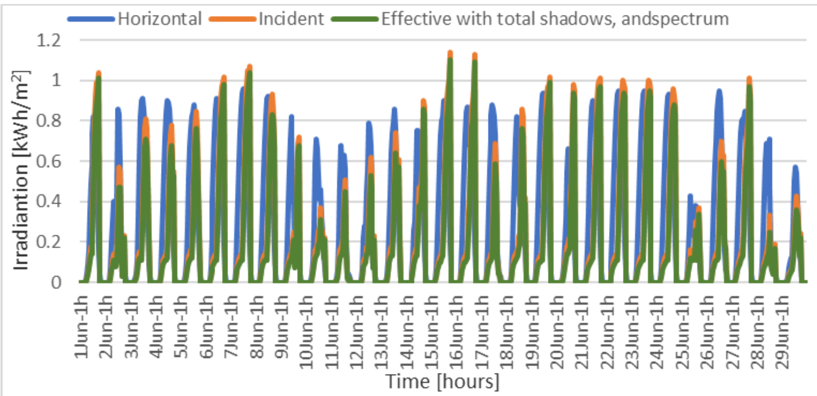

Fig. 4. Hourly Dynamics of Solar Energy Flux

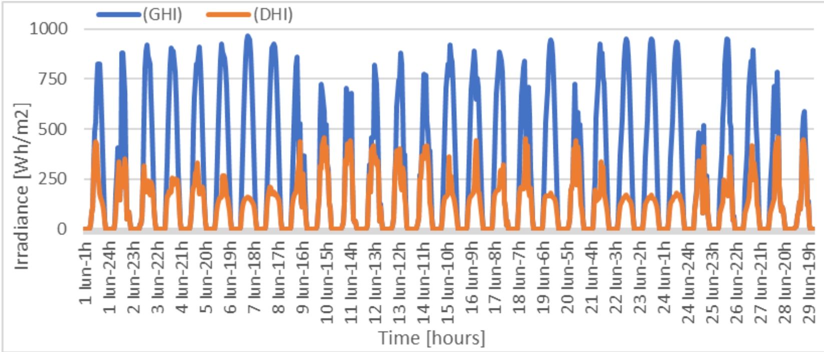

Fig. 5. Hourly evolution of Global Horizontal Irradiation (GHI, blue) and Diffuse Horizontal Irradiation (DHI, orange), representing total and diffused solar radiation on a horizontal surface.

To conclude, hourly representation is essential for an accurate and detailed assessment of PV system performance, while daily data provides a useful summary for general climate or energy evaluations.

B. Ambient temperature: This varies between approximately 17°C at night and 32–35°C in the afternoon, following a typical profile. Although useful for simulations, these data do not record the extreme events, such as heat waves, which can significantly reduce module performance by reducing the voltage.

Fig. 6 shows the hourly variation of background temperature for the reference month. Rising temperature reduces the efficiency of photovoltaic cells, a phenomenon pronounced in crystalline silicon (c-Si) technology, due to the increase the internal resistance that limits the flow of current. High ambient temperatures, above 30°C, decrease the terminal voltage, reducing the power and total energy delivered by the system. Thus, thermal effects represent a critical factor in evaluating and optimizing the global performance of the PV system.

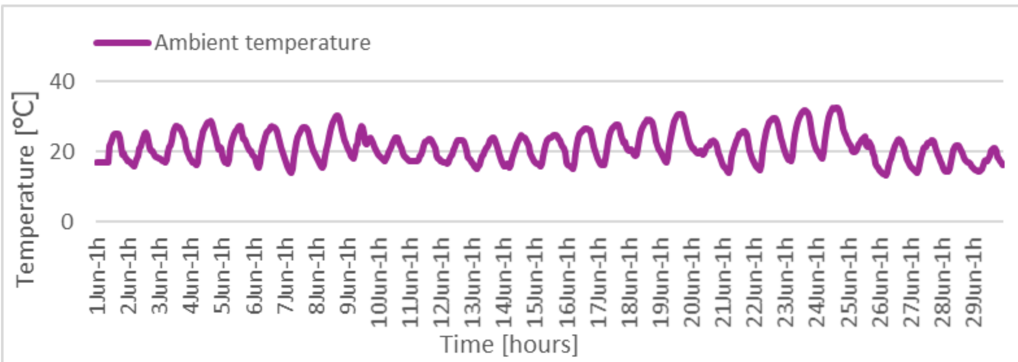

Fig. 6. Evolution of Ambient Temperature

Although ambient temperature values are useful for standard PV performance simulations, they do not capture real or extreme conditions, such as equipment overheating or atypical meteorological events. Therefore, integrating actual temperature measurements in PV system analysis is essential for adjusting temperature coefficients in the model, validating estimated efficiency, and attenuation losses through appropriate cooling or ventilation approach.

C. Wind speed and direction: According to Fig. 7, wind speed ranged from 0.5 to 6.5 m/s, while direction varied between 0 and 360°. In this case the wind plays a double role, namely: 1) it provides passive cooling of the panels, enhancing efficiency during hot days, and 2) it affects the structural design through mechanical loads. At high temperatures, cell performance decreases, but effective airflow induced by wind can lower panel temperatures and reduce thermal losses. At wind speeds of 3–5 m/s, improved efficiency can be achieved even under elevated ambient temperatures. Wind direction also influences the optimal orientation of panels and the design of appropriate protection systems for BIPV.

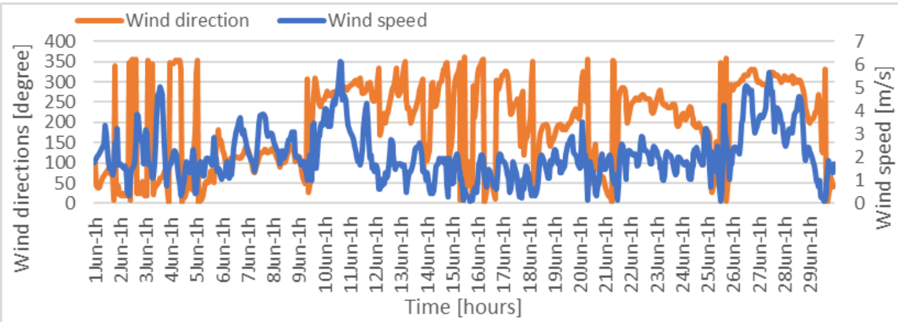

Fig. 7. Evolution of Wind Speed and Direction

In addition to irradiance and temperature, wind completes the model for predicting the actual performance of the system, exerting an indirect impact on the overall efficiency. On days with high irradiance and moderate wind (3–4 m/s), maximum net energy production is usually achieved.

To conclude, wind is an often-underestimated climatic factor, yet it plays an important role in evaluating the real behavior of photovoltaic systems.

3.2.Output Data: Energy Production

In this section, the authors analyzed the effective alternative current (AC) output, which closely follows the effective irradiance profile, including low irradiance and spectral effects, indicating a direct correlation between radiation availability and energy production. Days with high irradiance and moderate temperatures, combined with constant wind (June 7, 15, and 22), generated the highest daily performance (above 0.9 kWh/kWp/hour and 5 kWh/kWp daily), while days with persistent clouds and high temperatures (June 2, 11, and 25) significantly reduced production (below 0.3 kWh/kWp/hour and 2 kWh/kWp daily).

The DC versus AC curves indicate minimal conversion losses, and the overlap between AC output and effective irradiance suggests good efficiency under real-world conditions. Meteorological data remains an essential tool for simulation and initial sizing, but daily averages do not fully capture real-world variations. Hourly evaluation of irradiance, temperature and wind allows a more precise understanding of daily fluctuations, although losses caused by shading or panel fouling require further analysis. The combination of meteorological data and optimization techniques contributes to improving operational performance, model validation and increasing the stability of PV systems.

Fig. 8 shows the daily energy performance of the PV system during the period 1–29 June, expressed in kWh/kWp. The graph shows: the virtual DC yield at MPPT (theoretical maximum energy), the real DC yield at the panel terminals and the AC energy delivered to the consumer. The comparison highlights the system efficiency, the losses between the panel and the consumer and the MPPT performance. The PV generator reached high values on 1, 6–7, 15, 19 and 21–23 June, exceeding 4.5 kWh/kWp under favorable conditions.

Conversely, June 2, 10–11, 17, 25, and 28–29 is characterized by low performance, with values varying between 1.2 and 2.5 kWh/kWp, due to the cloud cover or other shading factors. The virtual DC curve consistently lies slightly above the real DC and AC curves, indicating minor losses due to system-related factors (temperature, orientation, soiling). The small difference between real DC and AC values reflects very high inverter efficiency and low conversion losses.

The next chapter proposes the use of MPPT algorithms for optimizing the overall performance of PV generators.

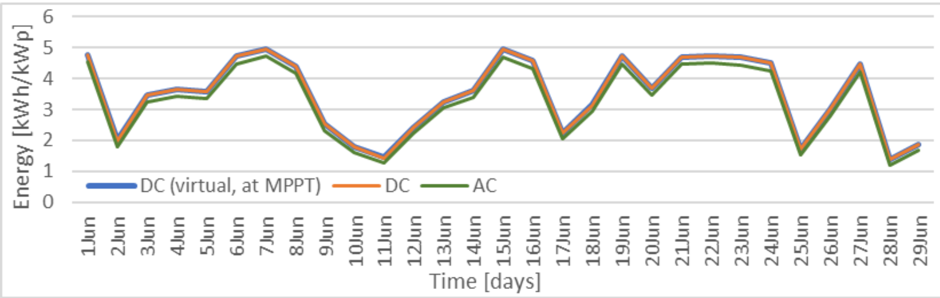

Fig. 8. Evolution of Daily Energy Production of the PV Generator

Pronounced day-to-day fluctuations in performance indicate a strong dependence on solar irradiance, emphasizing the need to integrate meteorological data into predictive models.

The results presented in Fig. 9 indicate that depending exclusively on daily data may introduce a positive bias in the estimation of PV system performance under real operating conditions. A detailed hourly analysis of energy production is essential for optimizing PV system sizing and preventing power losses. However, it is recommended to integrate real measurement data into simulation models based on MPPT optimization techniques, to achieve a more accurate performance.

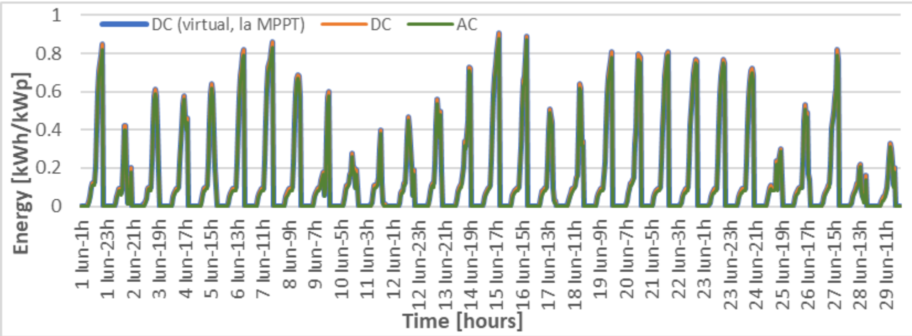

Fig. 9. Evolution of Hourly Energy Production of the PV Generator

4. Operational Optimization of PV Systems using MPPT Techniques

This chapter presents and discusses the results, which were analyzed to highlight the benefits of modeling and numerical simulation of photovoltaic (PV) systems, with a central focus on the adoption of Maximum Power Point Tracking (MPPT) techniques. This approach enabled a detailed investigation of the influence of partial shading on PV system performance, as well as an evaluation of the gain of MPPT algorithms in optimizing the conversion of solar energy into electrical energy.

Using a comprehensive MATLAB/SIMULINK-based modeling and simulation approach, the authors evaluated the energy performance of the PV generator and its adaptability under varying operating conditions. MPPT (Maximum Power Point Tracking) algorithms, such as Perturb and Observe with Fuzzy Logic Control (P&O FLC) and Incremental Conductance (INC), are suitable for maintaining the PV generator near its maximum power point under variable irradiance and temperature, optimizing total energy output.

Table 1 summarizes the simulation inputs, including meteorological conditions (solar irradiance, ambient temperature, wind speed), PV system electrical parameters (voltage, current, power), and total energy produced. Experimental data were correlated with simulation results in order to validate the MPPT models.

The study also examined two key factors: partial shading and bypass diode configuration. Simulations demonstrated that MPPT algorithms ensure stable maximum power point tracking; while shading and diode layout significantly affect system efficiency and energy yield by mitigating power losses and protecting the photovoltaic modules.

Table 1.

Experimental Data Corresponding to the Analyzed PV System

	Meteorological parameters			Electrical parameters				
Time step	**Irradia - nce** [W/m²]	**Temper - ature** [°C]	**Wind** [m/s]	**Power** [Wp]	**V_{mpp}** [V]	**I_{mpp}** [A]	**Energy** [Wh]	**Energy yield** [kWh/kW]
00:00:00	0.8	16.79	0.9	0.328	39	0.0084	0.328	0.0008
01:00:00	2.2	16.8	0.62	0.902	38.99	0.0231	0.902	0.0022
02:00:00	5.7	16.81	1.59	2.337	38.99	0.0599	2.337	0.0057
03:00:00	13.5	16.81	1.1	5.535	38.97	0.142	5.535	0.0135
04:00:00	29.3	16.82	1.17	12.013	38.93	0.3086	12.013	0.0293
05:00:00	58.7	16.83	1.66	24.067	38.85	0.6195	24.067	0.0587
06:00:00	108.3	16.83	2.62	44.403	38.73	1.1465	44.403	0.1083
07:00:00	184.1	16.84	1.24	75.481	38.54	1.9585	75.481	0.1841
08:00:00	288.4	16.85	1.45	118.244	38.28	3.0889	118.244	0.2884
09:00:00	416.4	21.6	2.28	170.724	37.96	4.4975	170.724	0.4164
10:00:00	554.1	22.53	3.38	227.181	37.61	6.0404	227.181	0.5541
11:00:00	679.5	25.18	3.03	278.595	37.3	7.469	278.595	0.6795
12:00:00	768	28.64	2.11	314.88	37.08	8.4919	314.88	0.768
13:00:00	850	29.75	3.86	348.5	37	9.4189	348.5	0.85
14:00:00	768	30.79	3.79	314.88	37.08	8.4919	314.88	0.768
15:00:00	679.5	30.82	2.28	278.595	37.3	7.469	278.595	0.6795
16:00:00	554.1	28.11	2.62	227.181	37.61	6.0404	227.181	0.5541
17:00:00	416.4	27.27	3.17	170.724	37.96	4.4975	170.724	0.4164
18:00:00	288.4	26.7	1.66	118.244	38.28	3.0889	118.244	0.2884
19:00:00	184.1	25.16	1.17	75.481	38.54	1.9585	75.481	0.1841
20:00:00	108.3	23.54	1.59	44.403	38.73	1.1465	44.403	0.1083
21:00:00	58.7	21.04	2.14	24.067	38.85	0.6195	24.067	0.0587
22:00:00	29.3	18.63	1.66	12.013	38.93	0.3086	12.013	0.0293
23:00:00	13.5	17.61	1.38	5.535	38.97	0.142	5.535	0.0135

4.1.Maximum Power Point Tracking Efficiency

The MPPT algorithms implemented for the PV generator successfully extracted the maximum available power, thus confirming the accuracy of the model. As shown in Fig. 10, a correlation can be observed between solar irradiance and the generated electrical energy, particularly in the time interval 11:00–14:00, when irradiance exceeds 600 W/m² and energy production reaches its highest levels. Under these conditions, the system maintains an almost constant operating voltage, around $V_{mp} \approx 37\text{–}38\,\text{V}$, while the current I_{mp} varies nearly linearly with solar irradiance. This indicates that the MPPT algorithm effectively adapts to rapid changes.

The maximum power reached is approximately 348.5 Wp at an irradiance level of 850 W/m², indicating high specific efficiency, typical for panels operating in the 17–20% efficiency range under ideal conditions.

4.2. PV System Behavior under Partial Shading Conditions and the Role of Bypass Diodes

A critical aspect in evaluating the performance of a photovoltaic system is how MPPT algorithms respond to both variations in solar irradiance and the presence of partial shading, a phenomenon frequently encountered in real applications. The analysis of the data presented in Fig. 10 highlights two relevant time intervals—09:00–11:00 and 15:00–17:00—during which variations in meteorological parameters, particularly the reduction in solar irradiance caused by partial shading, significantly affect electrical energy production.

During these intervals, although MPPT algorithms implement dynamic adjustments to keep the maximum power point, a decrease in generated energy is still observed, indicating inadequate tracking system performance.

In order to reduce this effect, the role of bypass diodes was also analyzed, as illustrated in Fig. 10 by automatically bypassing shaded cells, these diodes allow unaffected cells to continue operating, thereby preventing voltage drops and protecting system components.

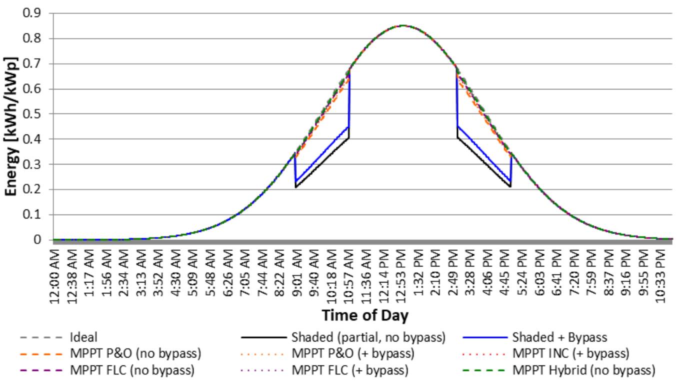

Fig. 10. Analysis of Electrical Energy Production under Partial Shading Conditions Using MPPT Optimization Techniques and Bypass Diodes

In the analysis of PV generator behavior under shading, it is essential to define clear thresholds: extreme shading occurs when more than 60% of the panel surface receives no direct solar irradiation. However, in the absence of bypass diodes, even localized shading affecting only 1–3% of the panel area (e.g., a few fully shaded cells) can significantly reduce power output, potentially leading to total energy loss. This is due to the series connection of cells, where the current is limited by the least illuminated cell. As illustrated in Fig. 11, without bypass diodes, no MPPT algorithm regardless of strategy can effectively recover or optimize energy production, as the system enters a constrained operating state caused by current limitation within the string.

By contrast, when bypass diodes are implemented to protect groups of cells (typically ~20 cells per diode), partial shading does not cause abrupt power drops. The affected diode becomes forward biased, bypassing the shaded section and allowing the remaining cells to continue operating. As a result, energy losses are limited, and the power curve remains relatively stable, enhancing system reliability under non-uniform shading conditions.

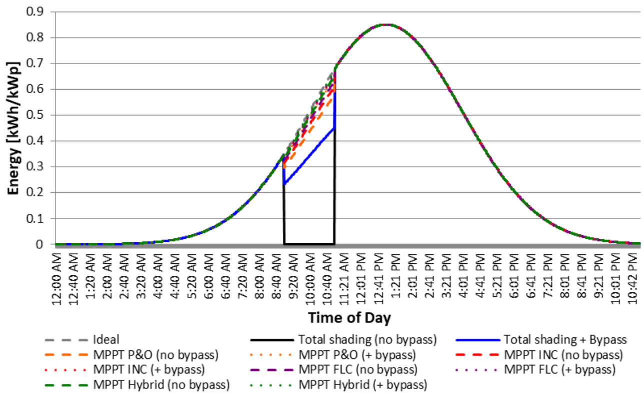

Fig. 11. Analysis of Electrical Energy Production under Extreme Shading Conditions Using MPPT Optimization Techniques and Bypass Diodes

5. Discussion and Conclusion

The results obtained in this study highlight the limitations of industrial software platforms in evaluating the performance of photovoltaic (PV) systems. Although these tools are useful for estimating annual yield, they typically generate overly optimistic forecasts because they fail to adequately capture system dynamics under partial shading conditions or during rapid fluctuations in meteorological parameters. Consequently, underestimation of the factors leading to system imbalances requires high-resolution modeling.

The transition to the MATLAB/Simulink environment has facilitated a much more detailed analysis at the component level. Simulations have demonstrated that the performance of both traditional and advanced maximum power point tracking (MPPT) techniques - such as Perturb and Observe (P&O), Incremental Conductance, and Fuzzy Logic Control - depend largely on irradiance uniformity. Although these methods effectively handle standard meteorological variations, the current study shows that, under severe partial shading conditions, the algorithms become inefficient. This inefficiency is caused by the distortion of the power-voltage (P-V) characteristic curve and the appearance of local maximum power points (LMPP), where algorithms risk converging incorrectly.

Furthermore, the analysis underlines the vital importance of hardware-software synergy. Bypass diodes act not merely as protective elements against the hot spot effect but actively reconfigure the circuit to limit power losses that the

MPPT alone could not recover. These findings indicate that, for practical implementations, numerical simulation must invariably be corroborated by experimental validation, thereby ensuring an accurate correlation between active and passive components, and control algorithms.

Given the challenges identified in managing non-uniform irradiance, future research directions will focus on photovoltaic systems using bifacial panels. In this context, modeling the capture of reflected radiation (albedo) will introduce new shading variables on the back side, requiring the development of even more robust control architectures to ensure both stability and efficiency.

Acknowledgements

The author, Ana-Maria Badea, gratefully acknowledges the financial support granted by the National University of Science and Technology POLITEHNICA Bucharest, Romania, in the form of a Ph.D. scholarship (Doctoral Contract No. SD12/4/02/10/2024).

R E F E R E N C E S

[1] *L. Fara, A. Diaconu, D. Craciunescu and S. Fara,* Forecasting of energy production for PV systems based on ARIMA and ANN advanced models, Int. J. Photoenergy, 1–19, 2021.
[2] *D. Craciunescu, L. Fara, P. Sterian, A. Bobei, F. Dragan*, Optimized Management for Photovoltaic Applications Based on LEDs by Fuzzy Logic Control and Maximum Power Point Tracking Springer International Publishing AG 2018 Nearly Zero Energy Communities Springer Proceedings in Energy, pp 317-336, 2018.
[3] *L. Fara, D. Craciunescu*, Output analysis of stand-alone PV systems: modeling simulation and control sustainable solutions for energy and environment, Energy Procedia 112, 595–605, 2017.
[4] *A. Barar, C. Boscornea, M. Balasoiu, D. Mănăilă-Maximean*, Two-diode modelling of perovskite solar cells and parameter extraction using the lambert w function, University Politehnica of Bucharest Scientific Bulletin-Series A-Applied Mathematics and Physics, 83(4), pp.285-294, ISSN 1223-7027, 2021.
[5] *S. Kataria, M. Kumar, A. Sikander,* A novel reconfiguration strategy for PV system under mismatch irradiance with experimental validation and machine learning-driven fault detection and diagnosis, Renewable Energy, Volume 261, 125323, ISSN 0960-1481, https://doi.org/10.1016/j.renene.2026.125323, 2026
[6] *A. Barar, D. Mănăilă-Maximean, M. Vlădescu, P. Schiopu*, Simulation of charge carrier transport mechanisms for quantum dot-sensitized solar cell structures, Univ. Politeh. Buchar. Ser. A 81, 265–270. ISSN 1223-7027, 2019.
[7] *L. Fara, A. Diaconu, D. Craciunescu,* Forecasting of energy production and operational optimization for photovoltaic systems, Ann. Acad. Romanian Scientists 3 (1), 31–60. ISSN 2559-1061, 2018.
[8] *A. Nazer, P. Manganiello, O. Isabella,* Hierarchical PV to PV series differential power processing for photovoltaic applications: Power flow and converter rating analysis, Mathematics and Computers in Simulation, Vol. 236, Pages 305-319, ISSN 0378-4754, 2025.
[9] *L. Fara, D. Craciunescu, S. Fara*, Numerical modelling and digitalization analysis for a photovoltaic pumping system placed in the south of Romania, Energies 14 (10) 2778, 2021.

[10] *A. Barar*, *D. Mănăilă-Maximean, C. Boscornea, M. Vlădescu, P. Schiopu*, Thermal behavior of the electrical parameters for a novel zinc derivativebased dye-sensitized solar cell. In: Advanced Topics in Optoelectronics, Microelectronics, and Nanotechnologies IX (Vol. 10977, pp. 177-181), SPIE, 2018.
[11] *M. Zhu, L. Yuan, H. Sun and P. Wu,* Nonlinear Sliding Mode Tracking Control for Maximum Power Point in Wind Turbine Generators, 2025 International Conference on Energy Power and Electrical Technology (CEPET), Wenzhou, China, pp. 131-136, doi: 10.1109/CEPET67280.2025.11390838, 2025.
[12] *L. Fara, A. Diaconu, D. Craciunescu*, Results in performance improvement and operational optimization of photovoltaic components and systems, Ann. Acad. Rom. Sci. Ser. Phys. Chem. Sci 2, 7–30. ISSN 2559-1061, 2017.
[13] *A. Barar, O. Dănilă, D. Mănăilă-Maximean, M. Vlădescu, P. Șchiopu*, Stochastic modelling of hopping charge carrier transport mechanism in organic photovoltaic structures. In Photonics for Solar Energy Systems VII (Vol. 10688, pp. 8-14), SPIE, 2018.
[14] *D. Crăciunescu, L. Fara*, Investigation of the Partial shading effect of photovoltaic panels and optimization of their performance based on high-efficiency FLC algorithm, Energies 16 (3), 1169, 2023.
[15] *E. C. Gouvêa, T. S. Castro, T. Miguel de Souza*, Performance analysis of interconnection and differential power processing techniques under partial shading conditions, Energies 17 (13), 3252,2024.
[16] *A.T. Altaye, P. Víg, I. Farkas*, Comparative analysis of photovoltaic system characteristics and performance through physical simulation, ANN modelling and experimental investigation. Discov Appl Sci 8, 192, https://doi.org/10.1007/s42452-025-08017-7, 2026.
[17] *A. Barar, D. Mănăilă-Maximean, O. Dănilă, M. Vlădescu*, Parameter extraction of an organic solar cell using asymptotic estimation and Lambert W function. In Advanced Topics in Optoelectronics, Microelectronics, & Nanotechnologies VIII (Vol. 10010, pp. 799-805). SPIE, 2016.
[18] *S. A. Pelaez, C. Deline, P. Greenberg, J. Stein, Raymond K.* Kostuk, Model and Validation of Single-Axis Tracking with Bifacial PV, Photovoltaic Energy Conversion (WCPEC-7) Waikoloa, Hawaii June 10–15, 2018.
[19] *H. Oufettoul, N. Lamdihine, S. Motahhir, N. Lamrini, I. A. Abdelmoula, G. Aniba*, Comparative Performance Analysis of PV Module Positions in a Solar PV Array Under Partial Shading Conditions, IEEE Access 11, 12176–12194, 2023.
[20] *H. Rezk, A. Fathy, A. Y. Abdelaziz*, A comparison of different global MPPT techniques based on metaheuristic algorithms for photovoltaic system subjected to partial shading conditions, Renew. Sustain. Energy Rev. 74, 377–386, 2017.
[21] *F. Belhachat, C. Larbes*, Photovoltaic array reconfiguration strategies for mitigating partial shading effects: recent advances and perspectives, Energy Conv. Manag. 313, 118547. ISSN 0196-8904, 2024.
[22] *F. Nicoletti, M. A. Cucumo, N. Arcuri*, Building-integrated photovoltaics (BIPV): a mathematical approach to evaluate the electrical production of solar PV blinds, Energy 263, ISSN 0360-5442, 2023.
[23] *L. Abad, S. Tamalouzt, K. Djermouni, S. Mekhilef, Y. Belkhier*, Analytical Modeling of Photovoltaic Systems Under Partial Shading Conditions Incorporating Bypass and Blocking Diodes Influence, International Journal of Energy Research, 2025, 3384091, 21 pages, https://doi.org/10.1155/er/3384091, 2025.
[24] *M.A. Qureshi, F. Torelli, S. Musumeci, A. Reatti, A. Mazza, G. Chicco*, A Novel Adaptive Control Approach for Maximum Power-Point Tracking in Photovoltaic Systems. Energies, 16, 2782. https://doi.org/10.3390/en16062782, 2023.

[25] *E. C. Lucchino, A. Gelesz, K. Skeie, G. Gennaro*, Modelling double skin façades (DSFs) in whole-building energy simulation tools: validation and inter-software comparison of naturally ventilated single-story DSFs, Build. Environ. 231, ISSN 0360-1323, 2024.
[26] *N. Karami, N. Moubayed, R. Outbib*, General review and classification of different MPPT Techniques, Renew. Sustain. Energy Rev. 68, 1–18. ISSN 1364-0321, 2017.
[27] *E.J. Kim, Y.H. Jeon, Y.C. Park, S.S. Park, S.J. Oh,* Evaluation of Photovoltaic Generation Forecasting Using Model Output Statistics and Machine Learning. Energies, 19, 486. https://doi.org/10.3390/en19020486, 2026.
[28] *AM. Badea, D. Mănăilă-Maximean, L. Fara, D. Craciunescu*, Maximizing solar photovoltaic energy efficiency: MPPT techniques investigation based on shading effects. Solar Energy, Volume 285, 113082, 2025.
[29] *V. Badescu*, Simple optimization procedure for silicon-based solar cell interconnection in a series–parallel PV module. Energy Conversion and Management 47, 1146–1158, 2006.
[30] *L. Fara, D. Crăciunescu, A. Diaconu, I. Chilibon, AM. Badea, S. Fara*, Advanced Architectural Integration of Aesthetic, Energetic and Reliable Features for Coloured Building Integrated Photovoltaic (BIPV) Systems, Environmental Engineering & Management Journal (EEMJ), Vol 23, Issue 3, p685, 2024.
[31] *** https://www.pvlighthouse.com.au/cms/simulation-programs/ (accessed February 20, 2026)
[32] *** http://www.sisifo.info/ (accessed February 20, 2026)